

In the format provided by the authors and unedited.

Phagocytosis-inspired behaviour in synthetic protocell communities of compartmentalized colloidal objects

Laura Rodríguez-Arco, Mei Li and Stephen Mann*

Centre for Protolife Research and Centre for Organized Matter Chemistry, School of Chemistry, University of Bristol, Bristol BS8 1TS, United Kingdom.

*email: laura.rodriquezarco@bristol.ac.uk, mei.li@bristol.ac.uk, s.mann@bristol.ac.uk

Supporting Information: Movies, Methods and Supplementary Figures and Notes

1. Supplementary Movies

Supplementary Movie 1.

Optical microscopy video showing magnetically directed movement and remote manipulation of a single MPE droplet (pH 10.2) within a population of cross-linked dye (carmine)-containing silica colloidosomes (red objects) dispersed in dodecane containing 1 mg mL⁻¹ oleic acid. Attachment of a single colloidosome to the MPE droplet followed by magnetically induced opening of the magnetite shell and slow ingestion of the colloidosome through the aperture is shown. Movie is shown at real-time speed. Individual frames showing the phagocytosis-like behaviour are shown in Fig 3a.

Supplementary Movie 2.

Optical microscopy video showing magnetically induced opening of the inorganic shell of a single MPE droplet (pH 10.2) located in a population of cross-linked silica colloidosomes (dyed red with encapsulated carmine) and dispersed in dodecane containing 1 mg mL⁻¹ oleic acid. Formation of fatty acid-stabilized patches increases the localized wetting behaviour on the polystyrene substrate such that neighbouring colloidosomes are engulfed. Removal of the magnetic field switches of the dynamical interactions and re-establishes a more isotropic particle distribution in the magnetite shell. Movie is shown at real-time speed.

Supplementary Movie 3.

Optical microscopy video showing spontaneous movement and phagocytosis-like behaviour of a single MPE droplet (pH 10.2) in a population of cross-linked silica colloidosomes (smaller objects) dispersed in dodecane containing 2 mg mL⁻¹ oleic acid. Self-propulsion and ingestion occur in the absence of the magnetic field. Note the high level of turbulence within their interior due to Marangoni convective flow along the interface. Movie is shown at real-time speed.

Supplementary Movie 4.

Optical microscopy video showing spontaneous phagocytosis-like behaviour of a single MPE droplet (pH 10.2) in a population of cross-linked silica colloidosomes (smaller objects) dispersed in dodecane containing 2 mg mL⁻¹ oleic acid. Movement

and phagocytosis are enhanced in the presence of the magnetic field. Note the high level of turbulence within their interior due to Marangoni convective flow along the interface. Movie is shown at real-time speed.

Supplementary Movie 5.

Optical microscopy video showing MPE droplets containing hydrophilic polystyrene beads and dispersed in a 2 mg mL^{-1} dodecane solution of oleic acid. Addition of the surfactant generates a high level of turbulence within the droplets due to Marangoni convective flow associated with mass transfer of oleate molecules through the oil/water interface. The beads follow ellipsoidal trajectories that exhibit bilateral symmetry within the droplet, and slow down with time as the system approaches equilibrium. No external magnetic field is applied. Movie is shown at real-time speed.

Supplementary Movie 6.

Optical microscopy video showing phagocytosis-like behaviour of a single MPE droplet (pH 10.2) located in a population of cross-linked silica colloidosomes containing 0.1 M NaCl solution (smaller objects) and dispersed in dodecane containing 2 mg mL^{-1} oleic acid. Movement and engulfment occur in the absence of a magnetic field. Note the low rate of colloidosome ingestion even though the fatty acid-stabilized aperture is in contact with the colloidosomes and despite the high level of turbulence in the MPE droplet interior. Movie is shown at real-time speed.

Supplementary Movie 7.

Fluorescence microscopy video showing spontaneous movement and phagocytosis-like behaviour of a single MPE droplet (pH 10.2) in a population of non-crosslinked silica colloidosomes (silica Pickering emulsion droplets) containing green fluorescent polystyrene beads (diameter = $3 \text{ }\mu\text{m}$). An external magnetic field is applied. Phagocytosis results in spontaneous disassembly of the silica-stabilized droplets and release of the microbeads into the interior aqueous phase of the MPE droplet. Note the high level of turbulence within the MPE droplet due to Marangoni convective flow. Movie is shown at real-time speed.

Supplementary Movie 8.

Fluorescence microscopy video showing engulfment-mediated enzymatic activity in a single ALP-containing MPE droplet accompanying ingestion of several silica colloidosomes comprising the small-molecule enzyme substrate fluorescein diphosphate. Release of the substrate followed by dephosphorylation and formation of fluorescein results in green fluorescence within the MPE droplet. No external magnetic field is applied. Movie is shown at real-time speed.

Supplementary Movie 9

Fluorescence microscopy video showing engulfment-mediated enzymatic activity in an ALP-containing MPE droplet. Six episodic colloidosome ingestion events are recorded for the MPE droplet under magnetic manipulation. In each event, formation of fluorescein results in an immediate increase in green fluorescence

followed by a slow decrease due to dilution inside the droplet. Movie is shown at real-time speed.

2. Supplementary Methods

Synthesis and characterization of magnetite particles. Magnetite particles were synthesized as follows according to previously reported procedure.¹ Briefly, 4.7 g of potassium hydroxide (purity $\geq 85\%$, Fisher Scientific, USA) and 14.2 g of potassium nitrate (purity $\geq 99\%$, Sigma-Aldrich, USA) were dissolved in 612 mL of deionized water previously purged for 2 h with nitrogen. In a separate container, sulphuric acid (44.0 μL , purity of 95%, VWR International, USA) and 12.2 g of iron sulphate heptahydrate (purity $\geq 99\%$, Sigma-Aldrich, USA) were dissolved in deionized water (44.4 mL) previously purged for 2 h with nitrogen. The solutions were subsequently mixed in a round-bottom flask to produce a dark green mixed-valence iron hydroxide precipitate. The mixture was then heated at 90 °C for 4 hours under a constant flow of nitrogen. As the reaction proceeded, the green precipitate turned black indicating the formation of magnetite particles. The mixture was finally allowed to cool and the precipitate was washed with deionized water until neutral pH using magnetic separation. The particles were stored in an inert atmosphere to prevent oxidation.

Samples of as-synthesized and partially hydrophobic magnetite were characterized by scanning electron microscopy (SEM; Jeol IT300, Japan) and X-ray diffraction (D8 Advance, Bruker UK Ltd) (data not shown).

Preparation of partially hydrophobic magnetite particles. Magnetite particles, *ca.* 500 nm in size, were synthesized as above, and functionalized with oleic acid to increase their surface hydrophobicity. For this, 0.5 g of the as-synthesized magnetite particles were dispersed in 25 mL of water by sonication, and 0.25 mL of oleic acid (neat liquid, purity $\geq 90\%$, Sigma-Aldrich, USA) added to give a pH of 5.0. The mixture was then heated at 80 °C for 15 min under mechanical stirring to give a dispersion of partially hydrophobic particles (pH = 4.3). The magnetite particles were separated magnetically, washed with water and then several times with acetone to remove any unbound oleic acid.

Engulfment of non-crosslinked silica colloidosomes. Experiments were undertaken with MPE droplets in the presence of non-crosslinked silica nanoparticle-stabilized water-in-oil droplets in place of the cross-linked silica colloidosomes. 200 μL of a dodecane suspension of silica nanoparticle-stabilized water-in-oil droplets (water/dodecane volume ratio = 0.05, silica/water weight ratio = 0.15) were prepared as previously described but without addition of tetramethoxysilane, and mixed with 1 mL of an oleic acid solution in dodecane (0.25–2.0 mg mL^{-1}). 20 μL of a water-in-dodecane magnetic Pickering emulsion (water/dodecane = 0.05, magnetite/water weight ratio = 0.1) prepared at pH 10.2 was then added and the mixed population imaged by optical and fluorescence microscopy.

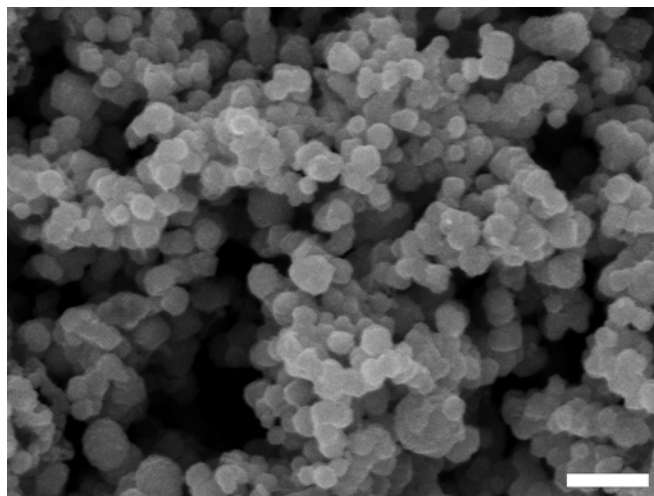
Contact angle and interfacial tension measurements. Contact angle measurements were performed using magnetite powders that were compressed into flat pellets with a smooth surface by the application of a force of 1×10^5 N for 5–10 minutes.

Contact angles of drops of water (volume of 0.2 μL) placed onto surface of the pellet were measured by the sessile drop method using a DSA100 tensiometer (Krüss, Germany). Each measurement was made in triplicate.

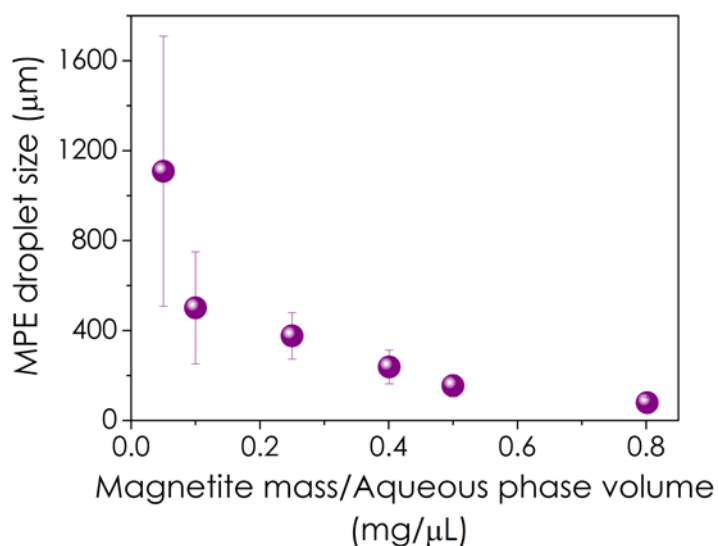
The interfacial tension between dodecane or oleic acid/dodecane solutions (0.001 - 2 mg mL^{-1}) and an aqueous phase (pH 5.5, 8.3, 10.2) was measured using the pendant drop method at 20 $^{\circ}\text{C}$ (DSA100 tensiometer). Drops of the aqueous solutions in oil were prepared using a syringe and monitored for 600-1800 s. Each measurement was made in triplicate, and the interfacial tension calculated from the Young-Laplace equation.

Oleic acid oil/water partitioning. Partitioning of oleic acid from dodecane into an aqueous solution prepared at different pH values was determined by measuring the initial and final concentrations of oleic acid in the oil after 24 h of contact with the aqueous solution. Briefly, 1 mL of an oleic acid solution in dodecane (concentration range: 0.25-1 mg mL^{-1}) was placed on top of 0.5 mL of an aqueous phase (pH 6-12) in a cylindrical flask (diameter of 1.5 cm). The oil phase was added slowly to the walls of the tube to avoid formation of dodecane droplets at the liquid interphase. The concentration of oleic acid in the oil phase at 25 $^{\circ}\text{C}$ was determined from the absorption band intensity at 235 nm using UV-Vis spectroscopy (Lambda 35 UV-Vis (Perkin Elmer), Peltier temperature controller). Each measurement was made in triplicate using three different stock solutions of oleic acid.

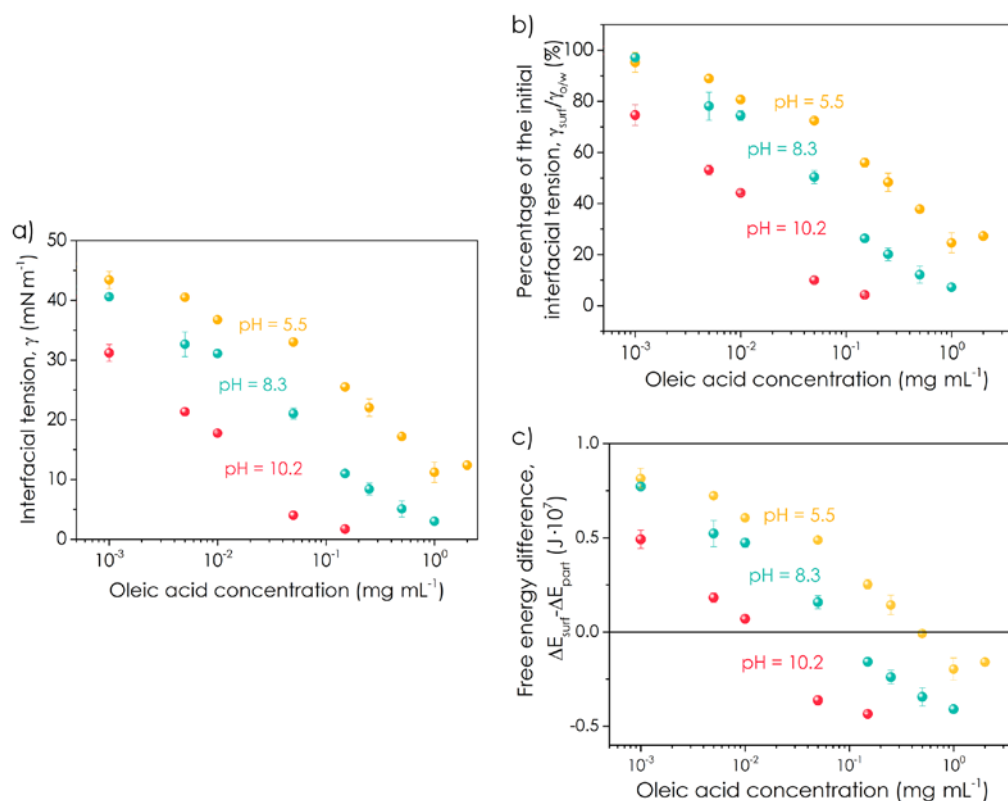
3. Supplementary Figures



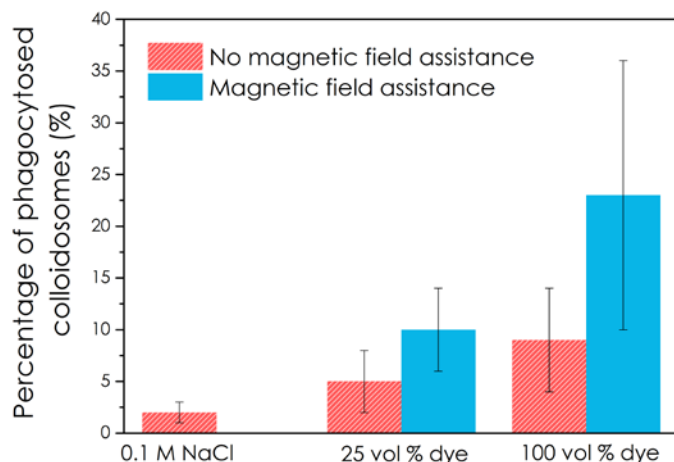
Supplementary Figure 1. Scanning electron microscopy image showing magnetite particles. Scale bar = 2 μm . The measured contact angle for water drops mounted on the surface of compressed powders of the oleate-capped magnetite was $\theta = 104.0 \pm 1.1^\circ$; corresponding measurements on non-coated magnetite powders was $11.4 \pm 1.4^\circ$.



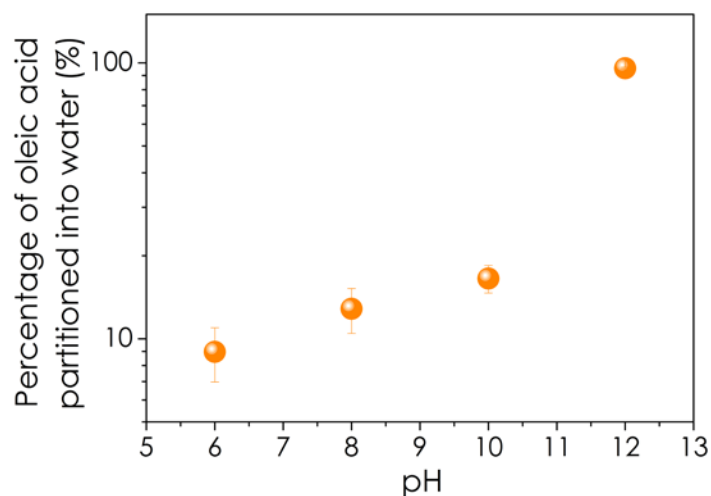
Supplementary Figure 2. MPE droplet diameter as a function of the ratio of magnetite mass to volume of the aqueous phase. Bars on data points represent standard deviations. The size and polydispersity of the droplets increased as the ratios decreased. Error bars correspond to standard deviations.



Supplementary Figure 3. (a) Plot of oil/water interfacial tension against oleic acid concentration in the oil phase for carbonate (pH = 10.2), Tris (pH = 8.3) and MES (pH = 5.5) buffered water droplets. The values of the interfacial tension for droplets formed in pure dodecane were 40.2 ± 0.3 mN m⁻¹ (pH = 10.2), 41.8 ± 0.3 mN m⁻¹ (pH = 8.3) and 45.6 ± 0.3 mN m⁻¹ (pH = 5.5). The interfacial tension decreased with increased oleic acid concentration, and was most strongly influenced at high pH. (b) Plot showing the ratio of the oil/water interfacial tension upon the addition of the surfactant (γ_{surf}) to its value in the absence of the surfactant ($\gamma_{\text{o/w}}$), $\gamma_{\text{surf}}/\gamma_{\text{o/w}}$, vs oleic acid concentration for water droplets at different pHs. Interfacial tensions were measured by the pendant drop method. (c) Corresponding plot of the difference in free energy variations between surfactant-stabilized and particle-stabilized emulsion droplets against oleic acid concentration at different pH values. See SI Note 1 for details of theoretical treatment. Error bars correspond to standard deviations.



Supplementary Figure 4. Plot showing percentage of silica colloidosomes ingested (“phagocytosed” by MPE droplets (pH = 10.2; oleic acid = 2 mg mL⁻¹) after 60 s with respect to the total number of colloidosomes in the field of view of the optical microscope. Data is shown for different solutes encapsulated within the colloidosomes, and the influence of remote manipulation by an external magnetic field is also displayed (blue columns). Aqueous dilution of the carmine dye increased the interfacial tension from $\gamma_{o/w} = 6.1 \pm 1.5$ mN m⁻¹ to 11.8 ± 0.9 mN m⁻¹, and produced a concomitant decrease in the phagocytosis rate measured over 60 s from 8 ± 5 % (undiluted) to 4 ± 2 %. Error bars correspond to standard deviations. Differences between values obtained for samples prepared at 25 or 100 vol % dye under the same magnetic field conditions, as well as between individual samples with or without magnetic field assistance were statistically significant ($p < 0.05$).



Supplementary Figure 5. Plot showing percentage of oleic acid transferred after 24 h from dodecane to an aqueous solution at different pHs. Values were determined by UV-Vis spectroscopy. The data correspond to the average values obtained for three different initial concentrations of oleic acid in the oil phase (0.25, 0.5 and 1 mg mL⁻¹). Error bars correspond to standard deviations.

4. Supplementary Notes

Free energy considerations for particle/surfactant exchange in Pickering emulsions

Addition of surfactant molecules to a particle-stabilized emulsion results in competition between the particles and the surfactant to occupy the interface. If the free energy variation difference between a surfactant- and particle-stabilized emulsion, $\Delta E_{\text{surf}} - \Delta E_{\text{part}}$ is negative, then the particles will be displaced from the interface. The free energy for a surfactant-stabilized emulsion is given by $\Delta E_{\text{surf}} = -4\pi R^2(\gamma_{\text{o/w}} - \gamma_{\text{surf}})$, where R is the radius of the emulsion droplet and $(\gamma_{\text{o/w}} - \gamma_{\text{surf}})$ is the difference in oil/water interfacial tension due to the presence of the surfactant. For a Pickering emulsion, the change in free energy is given by $\Delta E_{\text{part}} = -n\pi r^2\gamma_{\text{o/w}}(1 - |\cos\theta|)^2$, where n is the number of particles at the interface, r is their radius and θ is the contact angle with water. This expression can be simplified using the area fraction of the interface covered by spherical particles (ϕ) and by considering a contact angle (θ) of 90° . This gives $\Delta E_{\text{part}} = -4\pi R^2\gamma_{\text{o/w}}$, and the criterion for a surfactant-stabilized droplet to have a lower free energy than a particle-stabilized one becomes $(\gamma_{\text{o/w}} - \gamma_{\text{surf}})/\gamma_{\text{o/w}} > \phi$.² As a consequence, the relative reduction of the interfacial tension must be greater than the area fraction of the interface covered by particles.

We used measurements of the interfacial tension differences obtained from control experiments on adsorption of oleic acid at oil/water interfaces (Supplementary Fig. 3a,b) to determine the estimated values for $\Delta E_{\text{surf}} - \Delta E_{\text{part}}$ as a function of oleic acid concentration and droplet pH (Supplementary Fig. 3c). The plots indicated that the free energy variations became negative at lower concentrations of oleic acid as the pH was increased from 5.5 ($\approx 0.5 \text{ mg mL}^{-1}$) to 8.3 ($\approx 0.08 \text{ mg mL}^{-1}$) to 10.2 ($\approx 0.015 \text{ mg mL}^{-1}$), consistent with the differences in behaviour observed in Fig. 2j.

As shown in Supplementary Fig. 3c, displacement of the particles from the interface is predicted to occur at oleic acid concentrations as low as 0.015 mg mL^{-1} for the carbonate buffer system. However, we only observed significant changes of membrane fluidity for concentrations an order of magnitude higher. The theoretical predictions also suggested that instabilities should occur in MPE droplets prepared at pH 5.5 (MES buffer) for oleic acid concentrations of *ca.* 1 mg mL^{-1} (Supplementary Fig. 3c), but these were not detected. This disagreement between theory and our experimental observations can be attributed to the semi-quantitative nature of the theoretical analysis, which does not consider entropic contributions, attractive/repulsive interactions between the surfactant and the particles, or change of the contact angle with the addition of the surfactant.

Supplementary References

1. Gómez-Lopera, S. A., Plaza, R. C. & Delgado, A. V. Synthesis and Characterization of Spherical Magnetite/Biodegradable Polymer Composite Particles. *J. Colloid. Interface Sci.* **240**, 40-47 (2001).
2. Katepalli, H., John, V. T. & Bose, A. The response of carbon black stabilized oil-in-water emulsions to the addition of surfactant solutions. *Langmuir* **29**, 6790–6797 (2013).